

Nonlinear Optical Spectroscopy of Photonic Metamaterials

Evgenia Kim^{1,2*} and Feng Wang^{1,2}, Wei Wu³, Zhaoning Yu³, Yuen Ron Shen^{1,2}

*Department of Physics, University of California, Berkeley, CA, 94720*¹

*Material Science Division, Lawrence Berkeley National Laboratory, Berkeley, CA, 94720*² and

*Quantum Science Research, HP Labs, Hewlett-Packard, Palo Alto, CA, 94304*³

We have obtained spectra of second-harmonic generation, third harmonic generation, and four-wave mixing from a fishnet metamaterial around its magnetic resonance. The resonant behaviors are distinctly different from those for ordinary materials. They result from the fact that the resonance is plasmonic, and its enhancement appears through the local field in the nanostructure.

PACS numbers:

Optical metamaterials with nanoscale metal building blocks have been studied extensively in recent years [1]-[8]. With each metal unit much smaller than optical wavelength, they can be viewed as continuous media and the metal units act as 'artificial molecules'. The optical properties of metamaterials can be engineered by proper design of the 'artificial molecules' and they can exhibit unusual behavior nonexistent in nature, such as negative refractive indices. While linear optical properties of metamaterials have been well investigated [2]-[8], nonlinear optical properties began to attract interest only recently [9]-[19]. Such interest stems from possible strong enhancement of nonlinear response from plasmon resonances of the metal nanostructures together with spectral tunability offered by design of 'artificial molecules'. A crucial aspect in understanding nonlinear optical properties of metamaterials is their spectral responses, which have not yet been reported.

In this letter, we present the first spectroscopic study of second harmonic generation (SHG), third harmonic generation (THG) and four-wave mixing from a metamaterial comprising a monolayer of "fishnet" structure [20], [21]. It was designed to have negative refractive index in the near-IR range, with a magnetic resonance around $1.55 \mu\text{m}$ [22]. The spectra of SHG and THG with the fundamental input scanned over the magnetic resonance were obtained with different fundamental and harmonic polarizations. Resonant enhancement were clearly observed. Interestingly, the observed resonances are much sharper than that in linear absorption. This is distinctly different from typical molecular cases, where resonant excitation at the fundamental wavelength yields the same resonance spectrum in linear and nonlinear responses. Such difference originates from the fact that, unlike molecular resonances, the plasmon resonances in metal nanostructures are collective oscillations and their resonance enhancement appears through the local field effect in the nonlinear processes.

The measurements were carried out on a "fishnet" metamaterial composed of two silver sheets with hole arrays separated by a SiO_2 layer. It was fabricated us-

ing combination of nanoimprint lithography (NIL) and electron-beam lithography (EBL) [23]. The SEM image of the structure is shown in Fig. 1a and the structural configuration of the broad wire in Fig. 1b. Linear optical response of this metamaterial exhibits a magnetic resonance at $1.55 \mu\text{m}$ when the magnetic field component of the input wave threads the loop formed by linking the broad metal wires of the two layers, as indicated in Fig. 1b by the black arrows [24], [25]. Correspondingly, the effective refractive index is negative in the wavelength range of 1.45 to $1.6 \mu\text{m}$. The measured linear transmittance and reflectance spectra are presented in Fig. 1c.

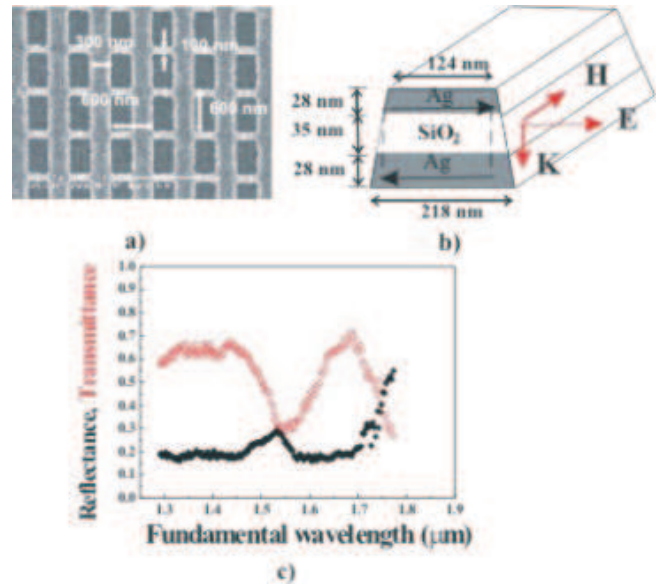


FIG. 1: a) SEM image of the fishnet structure; b) Schematic structure of the broad wire of "fishnet" $\text{Ag}/\text{SiO}_2/\text{Ag}$ structure. c) Linear transmittance (open dots) and reflectance (solid dots) spectra.

The nonlinear optical spectroscopy of the fishnet structure was performed using the tunable output from an optical parametric system, pumped by the third-harmonic of a picosecond YAG:Nd laser. The tunable IR beam was incident at 30° on the sample, and the reflected SHG, THG and four wave mixing signals were detected by a

*Electronic address: evgenia.kim@berkeley.edu

photo-multiplier and gated electronics system after spectral filtering.

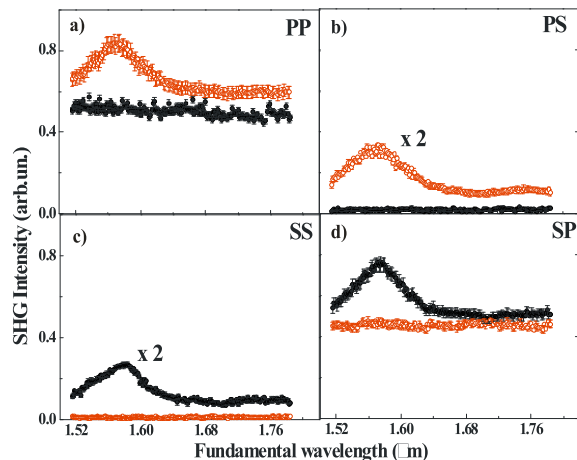


FIG. 2: SHG spectra of the fishnet structure for different polarization combinations: (a) p-in p-out, (b) p-in s-out, (c) s-in s-out, (d) s-in p-out. Solid dots and open dots are for beam geometry with the incident magnetic field component along and perpendicular to the broad Ag wire, respectively.

The SHG spectra, obtained with the incident plane along (solid dots) and perpendicular (open dots) to the broad Ag wires of the fishnet are shown in Fig. 2. Polarization combinations employed are indicated in the figure (PS, for example, denotes P and S polarizations for the fundamental input and SH output, respectively). To correct for the wavelength dependent incident laser intensity, the SHG signals at each wavelength were normalized to that of a smooth silver film with the PP polarization combination. Two features are clear in the SHG spectra. First, the SHG spectra display a resonance at $1.55 \mu\text{m}$ whenever the input polarization has a magnetic-field component along the broad wires of the fishnet (i.e., P- or S-polarized when the incident plane is perpendicular to or along the broad wires, respectively) and the magnetic resonance is excited. Otherwise, the SHG spectra are featureless with only non-resonant contribution. Second, the PS and SS polarizations yield weaker SHG signals with a much lower nonresonant background compared to PP and SP. Presumably this is the result of symmetry. As in the case of thin Ag films, SHG from a perfect fishnet structure, with the incident plane coinciding with a mirror plane, is strictly forbidden for PS and SS polarizations, but allowed for PP and SP. That SHG with SS and PS is actually observable is an indication that the fishnet sample is not ideally symmetric.

In Fig. 3, the THG spectra are shown for different sample orientations and polarization combinations using the same notations as those for SHG in Fig. 2. Strong en-

hancement of THG is observed when and only when the magnetic resonance is excited by the fundamental beam. The stronger signal for PP and SS compared with PS and SP polarization can also be understood from symmetry argument: THG with PS and SP is forbidden in a perfect fishnet structure when the incident plane coincides with a mirror plane. Compared with the SHG spectra, the non-resonant contribution is smaller in the THG signal and the resonance more pronounced.

We compare in Fig. 4 the magnetic resonant features in the PP spectra of linear absorption, SHG and THG. The resonance of THG is clearly narrower than that of SHG, which is in turn sharper than that of linear absorption. This is in striking contrast with molecular resonances, where resonance lineshapes of harmonic generation spectra are similar to that of linear absorption. It indicates that resonances of "artificial molecules" in metamaterials are characteristically different from those of natural molecules. The difference arises because plasmon resonances of metal nanostructures are intrinsically collective in nature instead of local as in molecular transitions. Such distinctions do not show up in linear optical properties, but become obvious in nonlinear optical spectra where a resonant input field participates multiple times in nonlinear processes. To further establish the above-mentioned characteristic resonant behavior in nonlinear responses of metamaterials, we measured outputs of four wave mixing at $3\omega_1$, $2\omega_1+\omega_2$ and $\omega_1+2\omega_2$ with ω_2 fixed (at wavelength of 1064 nm) and ω_1 scanned across the magnetic resonance. The observed spectra for PP polarization are displayed in Fig. 4b with signals at $2\omega_1+\omega_2$

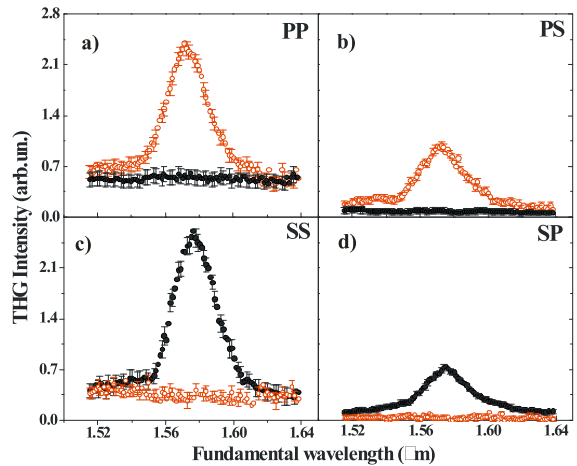


FIG. 3: THG spectra of the fishnet structure for different polarization combinations: (a) p-in p-out, (b) p-in s-out, (c) s-in s-out, (d) s-in p-out. Solid dots and open dots are for beam geometry with the incident magnetic field component along and perpendicular to the broad Ag wire, respectively.

and $\omega_1+2\omega_2$ scaled up by 6.6 and 43, respectively. It is

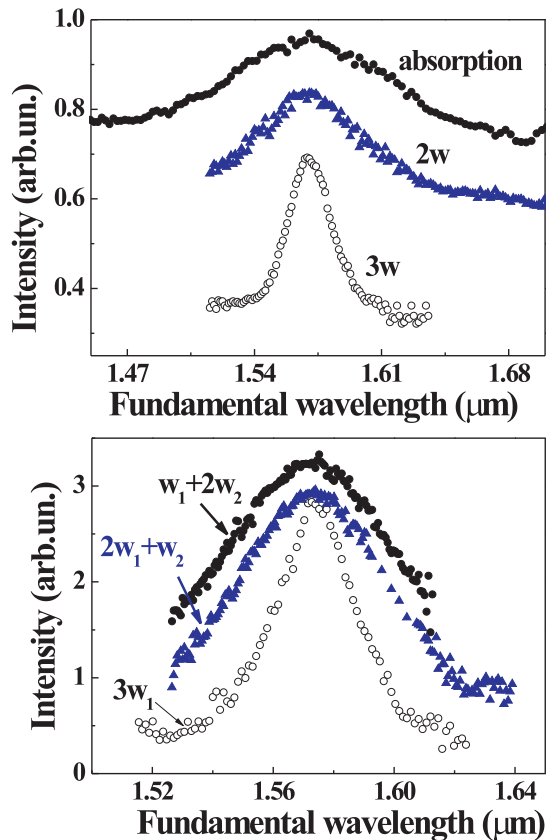


FIG. 4: a) Comparison of SHG (triangle) and THG (open dots) spectra in pp polarization combinations with the linear absorption spectrum (solid dots). b) Spectra of four-wave processes at $3\omega_1$ (open dots), $2\omega_1+\omega_2$ (triangles) and $\omega_1+2\omega_2$ (solid dots). The signal strengths at $2\omega_1+\omega_2$ and $\omega_1+2\omega_2$ are scaled up by 6.6 and 43, respectively, for ease of comparison.

obvious that each additional ω_1 component in the input leads to extra enhancement of the output at resonance, and the corresponding resonance peak becomes increasingly sharper.

For better understanding of the observed results, we realize that the real source of n th harmonic generation in metamaterials is the induced effective electric dipole on each nanostructural unit:

$$\vec{P}^{(n)} = \int_V \tilde{L}(\vec{r}, n\omega) : \tilde{\chi}^{(n)}(\vec{r}) : [\vec{E}_{loc}(\vec{r}, \omega)]^n dV, \quad (1)$$

where the integration is over the volume of the unit, $\tilde{\chi}^{(n)}$ is the local n th-order nonlinear susceptibility and $\vec{E}_{loc}(\vec{r}, \omega) = \tilde{L}(\vec{r}, \omega) : \vec{E}_0(\omega)$ is the local field with $\tilde{L}(\vec{r}, \omega)$ being the local field correction factor and $\vec{E}_0(\omega)$ the input field. For simplicity, we have neglected the contribution of magnetic-dipole and electric-quadrupole to $\vec{P}^{(n)}$

in Eq.(1). The harmonic output with polarization along \hat{n} is given by $S^{(n)} \propto |\hat{n} \cdot \vec{P}^{(n)}|^2$. The local field here can be decomposed into two components, one associated with the magnetic resonance and the other not. The resonant component is relatively enhanced when approaches resonance. Thus we can write the local field correction factor as $\tilde{L}(\vec{r}, \omega) = \tilde{A}(\vec{r}, \omega) + \tilde{B}(\vec{r}, \omega)/D(\omega)$ with D approximated by $D = \omega - \omega_0 + i\Gamma$ describing the magnetic plasmon resonance.

The symmetry requirement for harmonic generation is naturally incorporated in the volume integration of Eq.(1), which, for example, vanishes for symmetry forbidden processes in a perfect fishnet structure. The integral depends sensitively on the field distribution, and nonresonant and resonant terms respond differently to nanostructure change because of their different local field distributions: For a symmetry-forbidden harmonic generation process, if symmetry-breaking modification of the nanostructure is not severe, the nonresonant signal is still expected to be small. At resonance, however, $\tilde{B}(\vec{r}, \omega)$ being different from $\tilde{A}(\vec{r}, \omega)$ can have a spatial distribution emphasizing contribution from the symmetry-breaking part of the structure [26], thus generating a relatively strong resonant harmonic output. This explains our observation of resonant spectra with very weak nonresonant background for symmetry-forbidden harmonic generation processes in the fishnet structure presented in Figs. 2 and 3. Numerical calculation on a realistic fishnet structure hopefully will quantify the different effects of symmetry breaking on resonant and nonresonant harmonic generation.

If the nonresonant part of $\tilde{L}(\vec{r}, \omega)$ could be neglected, we would have, for the n th harmonic generation, $\vec{P}^{(n)} \propto |D|^{-n}$ and $S^{(n)} \propto |D|^{-2n}$. With the presence of the nonresonant $\tilde{A}(\vec{r}, \omega)$ term in $\tilde{L}(\vec{r}, \omega)$, the signal $S^{(n)}$ now has terms of $|D|^{-2m}$ with $m = 0, 1, \dots, n$, and its resonant lineshape often appears broader than $|D|^{-2n}$. However, the $|D|^{-2n}$ term is always significant, making the THG ($n = 3$) spectrum sharper than that of SHG ($n = 2$); similar behavior is seen in comparing spectra of wave mixing at $3\omega_1$, $2\omega_1+\omega_2$ and $\omega_1+2\omega_2$.

In summary, we have measured spectra of SHG, THG and four-wave mixing from a fishnet metamaterial around its magnetic resonance with different input/output polarization combinations. The results show that the resonant enhancement is much stronger in nonlinear optical response than that in the linear case, and the more times the resonant input field participates in the mixing process, the sharper the resonant spectrum appears to be. This is because the resonance is plasmonic in nature and shows up in the local-field correction factors in the nonlinear responses. Such resonant behavior is expected to appear in all nonlinear optical processes involving plasmon resonances in metamaterials.

Acknowledgments

This work was initiated under the sponsorship of DARPA. The authors were supported by Director, Office of Science, Office of Basic Energy Sciences, Materials Sci-

ences and Engineering Division, of the U.S. Department of Energy under Contract No. DE-AC03-76SF00098. FW acknowledges a fellowship support from the Miller Institute of the University of California.

-
- [1] J.B. Pendry, *Phys. Rev. Lett.* 85, 3966 (2000)
- [2] R.A. Shelby, D. R. Smith, and S. Schultz, *Science* 292, 77 (2001)
- [3] Y.J. Yen, W.J. Padilla, N. Fang, D.C. Vier, D.R. Smith, J.B. Pendry, D.N. Basov, X. Zhang, *Science*, 303, 1494 (2004)
- [4] S. Linden, C. Enkrich, M. Wegener, J. Zhou, Th. Koschny, and C. M. Soukoulis, *Science* 306, 13511353 (2004).
- [5] V. M. Shalaev, W. Cai, U. K. Chettiar, H.-K. Yuan, A. K. Sarychev, V. P. Drachev, and A. V. Kildishev, *Opt. Lett.* 30, 33563358 (2005).
- [6] Shalaev V.M., *Nature Photonics*, v.1, 41-48 (2007)
- [7] C. M. Soukoulis, S. Linden, and M. Wegener, *Science* 315, 4749 (2007).
- [8] G. Dolling et al., *Opt. Lett.* 32, 53 (2007)
- [9] M.W. Klein, C. Enkrich, M. Wegener, S. Linden, *Science* 313, 502 (2006)
- [10] M.W. Klein, M. Wegener, N. Feth, S. Linden, *Optics Express* 15, 5238 (2007)
- [17] A. A. Zharov, I. V. Shadrivov, and Y. S. Kivshar, *Phys. Rev. Lett.* 91, 037401 (2003).
- [12] S. O'Brien, D. McPeake, S. A. Ramakrishna, and J. B. Pendry, *Phys. Rev. B* 69, 241101(R) (2004).
- [13] A. K. Popov, V. V. Slabko, and V. M. Shalaev, *Las. Phys. Lett.* 3, 293297 (2006).
- [14] A. K. Popov and V. M. Shalaev, *Appl. Phys. B* 84, 131137 (2006).
- [15] A. K. Popov and V. M. Shalaev, *Opt. Lett.* 31, 21692171 (2006).
- [16] M. V. Gorkunov, I. V. Shadrivov, and Y. S. Kivshar, *Appl. Phys. Lett.* 88, 71912 (2006).
- [17] A. A. Zharov, N. A. Zharova, I. V. Shadrivov, and Y. S. Kivshar, *Appl. Phys. Lett.* 87, 091104 (2005).
- [18] R. S. Bennink, Y.-K. Yoon, and R. W. Boyd, *Opt. Lett.* 24, 14161418 (1999).
- [19] J. P. Huang, L. Dong, and K. W. Yu, *J. Appl. Phys. B* 99, 053503 (2006).
- [20] S. Zhang et al., *Opt. Exp* 13, 4922 (2005).
- [21] S. Zhang, W. Fan, N. C. Panoiu, K. J. Malloy, R. M. Osgood, and S. R. J. Brueck, *Phys. Rev. Lett.* 95, 137404 (2005).
- [22] W.Wu*, E.Kim*, E.Ponizovskaya et.al., *Appl. Phys. A* 87, 143 (2007).
- [23] W. Wu, Y.M. Liu, E. Kim et.al., *Appl. Phys.Lett.* 90, 063107 (2007)
- [24] A.N. Lagarkov and A. K. Sarychev, *Phys. Rev. B* 53, 6318 (1996);
- [25] V.A. Podolskiy, A.K. Sarychev, and V.M. Shalaev, *Opt. Express* 11, 735 (2003)
- [26] For the SS case with incident plane along the broad Ag wire, for example, it can be seen that the resonant field distribution emphasizes the field at the edges of the wires where the symmetry breaking occur, but the nonresonant field distribution does not.